Transform-Invariant Convolutional Neural Networks for Image Classification and Search

Xu Shen
CAS Key Laboratory of
Technology in Geo-spatial
Information Processing and
Application System
University of Science and
Technology of China
Hefei, Anhui, China 230027
shenxu@mail.ustc.edu.cn

Xinmei Tian
CAS Key Laboratory of
Technology in Geo-spatial
Information Processing and
Application System
University of Science and
Technology of China
Hefei, Anhui, China 230027
xinmei@ustc.edu.cn

Anfeng He
CAS Key Laboratory of
Technology in Geo-spatial
Information Processing and
Application System
University of Science and
Technology of China
Hefei, Anhui, China 230027
heanfeng@mail.ustc.edu.cn

Shaoyan Sun
CAS Key Laboratory of
Technology in Geo-spatial
Information Processing and
Application System
University of Science and
Technology of China
Hefei, Anhui, China 230027
sunshy@mail.ustc.edu.cn

Dacheng Tao
Centre for Quantum
Computation & Intelligent
Systems and the Faculty of
Engineering and Information
Technology
University of Technology,
Sydney
Ultimo, NSW 2007, Australia
dacheng.tao@uts.edu.au

ABSTRACT

Convolutional neural networks (CNNs) have achieved state-of-the-art results on many visual recognition tasks. However, current CNN models still exhibit a poor ability to be invariant to spatial transformations of images. Intuitively, with sufficient layers and parameters, hierarchical combinations of convolution (matrix multiplication and non-linear activation) and pooling operations should be able to learn a robust mapping from transformed input images to transform-invariant representations. In this paper, we propose randomly transforming (rotation, scale, and translation) feature maps of CNNs during the training stage. This prevents complex dependencies of specific rotation, scale, and translation levels of training images in CNN models. Rather, each convolutional kernel learns to detect a feature that is generally helpful for producing the transform-invariant answer given the combinatorially large variety of transform levels of its input feature maps. In this way, we do not require any extra training supervision or modification to the optimization process and training images. We show that random transformation provides significant improvements of CNNs on many benchmark tasks, including small-scale image recognition, large-scale image recognition, and image retrieval.

Permission to make digital or hard copies of all or part of this work for personal or classroom use is granted without fee provided that copies are not made or distributed for profit or commercial advantage and that copies bear this notice and the full citation on the first page. Copyrights for components of this work owned by others than ACM must be honored. Abstracting with credit is permitted. To copy otherwise, or republish, to post on servers or to redistribute to lists, requires prior specific permission and/or a fee. Request permissions from permissions@acm.org.

MM'16, October 15–19, 2016, Amsterdam, The Netherlands.

© 2016 ACM. ISBN 978-1-4503-3603-1/16/10...$15.00

DOI: http://dx.doi.org/10.1145/264284.2964316

Keywords

Convolutional Neural Networks; transform invariance.

1. INTRODUCTION

In recent years, computer vision has been significantly advanced by the adoption of convolutional neural networks (CNNs). We are currently witnessing many CNN-based models achieving state-of-the-art results in many vision tasks, including image recognition [35, 32, 17, 8, 36], semantic segmentation [14], image captioning [19, 4, 5], image retrieval [40, 41, 39], action recognition [11, 31], video concept learning [7, 9] and video captioning [38, 28].

The local transform-invariant property of CNNs lies in the combination of local receptive fields with shared weights and pooling. Because distortions or shifts of the input can cause the positions of salient features to vary, local receptive fields with shared weights are able to detect invariant elementary features despite changes in the positions of salient features [24]. Moreover, average-pooling or max-pooling reduces the resolution of the feature maps in each layer, which reduces the sensitivity of the output to small local shifts and distortions. However, due to the typically small local spatial support for pooling (e.g., 2×2 pixels) and convolution (e.g., 9×9 kernel size), large global invariance is only possible for a very deep hierarchy of pooling and convolutions, and the intermediate feature maps in CNNs are not invariant to large transformations of the input data [25]. This limitation of CNNs results from the poor capacity of pooling and the convolution mechanism in learning global transform-invariant representations (Fig. 1).

In this work, we introduce a random transformation module of feature maps that can be included in any layer in a CNN. Intuitively, with sufficient layers and parameter-

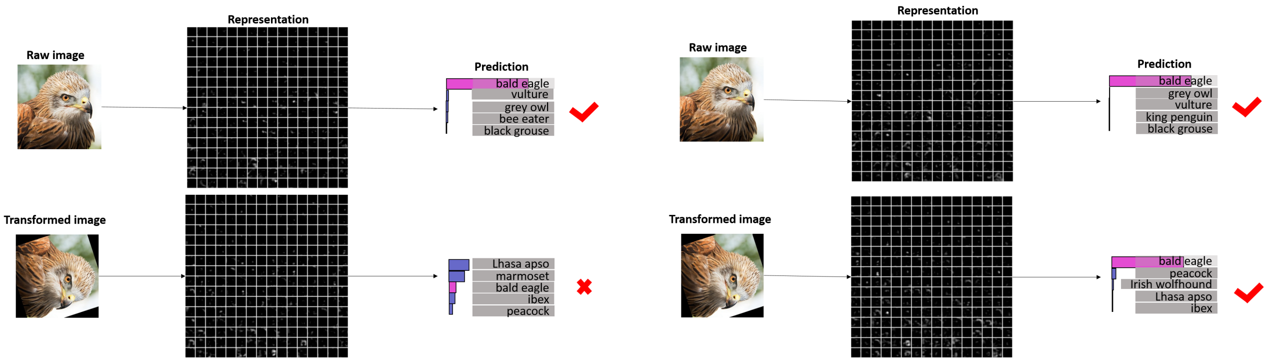

(a) CNN

(b) Transform Invariant CNN

Figure 1: Limitation of current CNN models. The length of the horizontal bars is proportional to the probability assigned to the labels by the model, and pink indicates ground truth. Transform of input image causes the CNN to produce an incorrect prediction (a). Additionally, the representations ($256 \times 14 \times 14$ conv5 feature maps of AlexNet [21]) are quite different, while the representation and prediction of our transform-invariant CNN (same architecture as [21]) is more consistent (b).

s, hierarchical combinations of convolution (matrix multiplication and non-linear activation) and pooling operations should have sufficient complexity to learn a robust mapping from input images with any transform to transform-invariant representations. All we need is to introduce a global way to push the CNN to learn with little dependency on the transform of input images. Our method is inspired by the success of dropout [27]. In dropout, each hidden unit is randomly omitted from the network with a probability (e.g., 0.5) on each presentation of each training case. Therefore, a hidden unit cannot rely on other hidden units being present. In this way, each neuron learns to detect a independent feature that is generally robust for producing the correct answer with little dependency on the variety of internal contexts in the same layer. Similarly, randomly transforming (rotation, scale, and translation) feature maps of CNNs during the training stage prevents complex dependencies of specific rotation, scale, and translation levels of training images in CNN models. Rather, each convolutional kernel learns to detect a feature that is generally helpful for producing the transform-invariant answer given the combinatorially large variety of transform levels of its input feature maps.

In contrast to pooling layers, in which receptive fields are fixed and local, the random transformation is performed on the entire feature map (non-locally) and can include any transformation, including scaling, rotation, and translation. This guides the CNN to learn global transformation-invariant representations from raw input images. Notably, CNNs with random transformation layers can be trained with standard back-propagation, allowing for end-to-end training of the models in which they are injected. In addition, we do not require any extra training supervision or modification of the optimization process or any transform of training images.

The main contributions of this work are as follows. (i) We propose a very simple approach to train robust transform-invariant convolutional neural networks. (ii) Because our model does not possess any extra parameters or extra feature extraction modules, it can be used to replace traditional CNNs in any CNN-based model. Therefore, this is a general approach for improving the performance of CNN-based models in any vision task. (iii) The validity of our method confirms that CNNs still have the potential to model a more robust mapping from transform-variant images to transform-invariant representations; we just need to push them to do so.

The remainder of this paper is structured as follows. Related works of transform-invariant CNNs are discussed in Section 2. The architecture and learning procedure of the proposed transform-invariant CNNs are described in Section 3. Extensive evaluations compared with the state-of-the-art and comprehensive analysis of the proposed approach are reported in Section 4. Conclusions are presented in Section 5.

2. RELATED WORK

The equivalence and invariance of CNN representations to input image transformations were investigated in [34, 3, 10]. Specifically, Cohen and Welling [3] showed that the linear transform of a good visual representation was equivalent to a combination of the elementary irreducible representations by using the theory of group representations. Lenc and and Vedaldi [25] estimated the linear relationships between representations of the original and transformed images. Gens and Domingos [10] proposed a generalization of CNN that forms feature maps over arbitrary symmetry groups based on the theory of symmetry groups in [34], resulting in feature maps that were more invariant to symmetry groups. Bruna and Mallat [2] proposed a wavelet scattering network to compute a translation-invariant image representation. Local linear transformations were adopted in feature learning algorithms in [33] for the purpose of transformation-invariant feature learning.

Many recent works have focused on introducing transformation invariance in deep learning architectures explicitly. For unsupervised feature learning, Sohn and Lee [33] presented a transform-invariant restricted Boltzmann machine that compactly represented data by its weights and their transformations, which achieved invariance of the feature representation via probabilistic max pooling. Each hidden unit was augmented with a latent transformation assignment variable that described the selection of the transformed view of the weights associated with the unit in [20]. In these two works, the transformed filters were only applied at the center of the largest receptive field size. In tied convolutional neural works [23], invariances were learned explicitly by square-root pooling hidden units that were computed by partially un-tied weights. Here, additional learned parameters were needed when un-tying weights. Alvarez *et al.* [1] learned each ConvNet over multiple scales independently without weight sharing and fused the outputs of these ConvNets. Sermanet and LeCun [30] utilized multi-scale CNN features by feeding the outputs of all the convolutional layers to the classifier. In these two models, multiple-scale information was captured from different levels or models of the hierarchy, but scale invariance was not encoded in the features learned at a layer because each layer is only applied to the original scale. In [6], the raw input image was transformed through a Laplacian pyramid. Each scale was fed into a 3-stage convolutional network, which produces a set of feature maps with different scales disjointly. Then, the outputs of all scales were aligned by up-sampling and concatenated. However, concatenating multi-scale outputs to extract scale-independent features involves extra convolution models and extra parameters, thereby increasing the complexity of the models and the computational cost.

The latest two works on incorporating transform invariance in CNNs are described in [18, 15]. In [18], feature maps in CNNs were scaled to multiple levels, and the same kernel was convolved across the input in each scale. Then, the responses of the convolution in each scale were normalized and pooled at each spatial location to obtain a locally scale-invariant representation. In this model, only limited scales were considered, and extra modules were needed in the feature extraction process. To address different transformation types in input images, [15] proposed inserting a spatial transformer module between CNN layers, which explicitly transformed the input image into the proper appearance and fed that transformed input into CNN model. In this work, invariance comes from the extra transformation module, while invariance of the CNN itself is not improved.

In conclusion, all the aforementioned related works improve the transform invariance of deep learning models by adding *extra feature extraction modules*, *more learnable parameters* or *extra transformations on input images*, which makes trained CNN models problem dependent and not easy to be generalized to other datasets. In contrast, in this paper, we propose a very simple random transform operation on feature maps during the training of CNN models. Intrinsic transform invariance of the current CNN model is obtained by pushing the model to learn more robust parameters from raw input images only. No extra feature extraction modules or more learnable parameters are required. Therefore, it is very easy to apply the trained transform-invariant CNN model to any vision task because we only need to replace current CNN parameters by this trained model.

3. TRANSFORM-INVARIANT CONVOLUTIONAL NEURAL NETWORKS

3.1 Convolutional Neural Networks

Convolutional neural networks (CNNs) are a supervised feed-forward multi-layer architecture in which each layer learns a representation by applying feature detectors to previous feature maps. The outputs of the final layer are fed into a classifier or regressor with a target cost function such that the network can be trained to solve supervised tasks. The entire network is learned through stochastic gradient descent with gradients obtained by back-propagation [24]. In general, a layer in a CNN consists of local patch-based linear feature extraction and non-linear activation, occasionally followed by spatial pooling or normalization.

The core concept of CNNs is a combination of local receptive fields, shared weights, and spatial pooling. Each unit in a layer receives inputs from a set of units located in a small neighborhood in the previous layer. This idea of connecting units to local receptive fields is inspired by Wiesel's discovery of locally sensitive and orientation-selective neurons in the visual system of cats [24]. The output of convolving an input layer with one kernel is called a *feature map*. Because elementary feature detectors (convolutional weights) that are useful on one part of the image should also be useful across the entire image, units in the same feature map share the same set of weights at multiple locations. This is a good way to reduce the number of trainable parameters and ensure some local shift and distortion invariance. Pooling is a simple way to reduce the spatial resolution of the feature map and also reduces the sensitivity of convolution outputs to shifts and distortions.

In the forward pass of a CNN, each output feature map is computed by convolving input feature maps with kernel weights and then activated by a non-linear activation function:

$$x_j^l = f((W_j^l * x^{l-1}) + b_j^l) \tag{1}$$

where $*$ is the convolution operator, x^{l-1} is the input feature maps from the previous layer, and f is a non-linear function. W_j^l and b_j^l are the trainable weights and bias of jth output feature map x_j^l.

3.2 Transformation of an Image

The basic 2D transformation of an image consists of 3 types: *translation*, *rotation*, and *scale* [29]. The locations of pixels in an image before transformation and after transformation are denoted as (x, y) and (x', y'), respectively. Translation is calculated by:

$$(x', y', 1) = (x, y, 1)\begin{bmatrix} 1 & 0 & 0 \\ 0 & 1 & 0 \\ d_x & d_y & 1 \end{bmatrix} \tag{2}$$

where d_x and d_y are the numbers of translated pixels in the x and y axes, respectively.

Scale is computed by:

$$(x', y', 1) = (x, y, 1)\begin{bmatrix} s_x & 0 & 0 \\ 0 & s_y & 0 \\ 0 & 0 & 1 \end{bmatrix} \tag{3}$$

where s_x and s_y are the scale factors in the x and y axes, respectively.

Rotation is computed by:

$$(x', y', 1) = (x, y, 1)\begin{bmatrix} cos\theta & sin\theta & 0 \\ -sin\theta & cos\theta & 0 \\ 0 & 0 & 1 \end{bmatrix} \tag{4}$$

where θ is the rotation angle ranging from -180° to 180°.

When translation, scale, and rotation are applied to an image simultaneously, the output can be computed as:

$$(x', y', 1) = (x, y, 1) \begin{bmatrix} cos\theta & sin\theta & 0 \\ -sin\theta & cos\theta & 0 \\ 0 & 0 & 1 \end{bmatrix} \begin{bmatrix} s_x & 0 & 0 \\ 0 & s_y & 0 \\ 0 & 0 & 1 \end{bmatrix} \begin{bmatrix} 1 & 0 & 0 \\ 0 & 1 & 0 \\ d_x & d_y & 1 \end{bmatrix} \tag{5}$$

3.3 Transform-Invariant Convolutional Neural Networks

Weight sharing makes CNN capable of detecting features regardless of their spatial locations in the input feature maps. Pooling reduces the sensitivity of CNN to local shifts and distortions in input images. However, when faced with global transformations of input images, the performance of CNNs is significantly decreased. In this section, we describe our transform-invariant CNN (TICNN). By introducing random transformations (scale, rotation, and translation) of feature maps in the CNN model, convolutional kernels are trained to be invariant to these transformations. Fig. 2 presents a side-by-side comparison of the overall structure of these two CNN layers.

One perspective to interpret TICNN is to compare it with dropout [27]. Dropout attempts to introduce a neuron-level randomness to deep models; in this way, the dependency of the feature detector on the existence of neurons in the same layer is reduced. TICNN attempts to incorporate a feature map (concept)-level randomness in CNN models, which can reduce the dependence of feature detectors in the current layer on the transform level of previous feature maps (appearance).

From the perspective of transformation, Jaderberg *et al.* [15] proposed transforming the input into a proper and easy-to-recognize appearance. TICNN forces the architecture to learn a more robust model for all possible transformations, and the intrinsic transform invariance of the architecture is improved.

From the perspective of data augmentation, training data augmentation and multi-scale model augmentation [18, 6] only provide the model with limited transform levels of input images or feature maps. While in TICNN, as training proceeds, the model will learn almost all transformation levels of inputs randomly. Therefore, TICNN should be more robust when input images are transformed.

Considering the spatial range of transformation invariance, pooling can only address a local invariance for shifts and distortions (e.g., 3 × 3 pixels). Our TICNN paves the way for global invariance of transformations in CNN models.

3.3.1 Forward Propagation

Our goal is to push each feature detector to learn a feature that is generally helpful for producing the transform-invariant answer given a large variety of transform levels of its input feature maps. To accomplish this goal, before being convolved by the convolutional kernels/filters, the input feature maps are first scaled, rotated and translated via a random sampled scale factor, rotation angle and translate proportion. To keep the size of feature maps unchanged, the transformed feature maps are either cropped or padded with 0s to be properly convolved.

Specifically, let $\mathcal{T}$ be a linear image transform operator that applies random spatial transformations to an input x. The output feature map y is computed as:

$$\hat{x} = \mathcal{T}(x) \tag{6}$$

$$y = f((W * \hat{x}) + b) \tag{7}$$

Here, the 3×3 transformation matrix $\mathcal{T}$ is randomly sampled as follows:

$$\mathcal{T} = \begin{bmatrix} cos\theta & sin\theta & 0 \\ -sin\theta & cos\theta & 0 \\ 0 & 0 & 1 \end{bmatrix} \begin{bmatrix} s_x & 0 & 0 \\ 0 & s_y & 0 \\ 0 & 0 & 1 \end{bmatrix} \begin{bmatrix} 1 & 0 & 0 \\ 0 & 1 & 0 \\ d_x & d_y & 1 \end{bmatrix} \tag{8}$$

where $\theta \sim \mathcal{N}(\mu_\theta, \sigma_\theta^2)$, $s_x, s_y \sim \mathcal{N}(\mu_s, \sigma_s^2)$, and $d_x, d_y \sim \mathcal{N}(\mu_d, \sigma_d^2)$. In the presence of each training image, $\{\theta$, s_x, s_y, d_x, and $d_y\}$ are randomly sampled.

3.3.2 Back-Propagation

Because the transform-invariant convolution layer consists of only linear operations, its gradients can be computed by a simple modification of the back-propagation algorithm. For each transformation, the error signal is propagated through the bilinear coefficients used to compute the transformation.

Let x^{l-1} denote the vectorized input of layer l of length m ($m = hwc$ for a h by w by c image). If the dimensionality of the transformed output is n, the transformation $\mathcal{T}$ of input x^{l-1} can be computed via Tx^{l-1}, where T is an $n \times m$ interpolation coefficient matrix. Specifically, each row of T has 4 non-zero coefficients with bilinear interpolation. By encoding kernel weights W as a Toeplitz matrix, the convolution operation can be expressed as:

$$z^l = toep(W)(Tx^{l-1}) + b^l \tag{9}$$

$$x^l = f(z^l) \tag{10}$$

where f is a non-linear function and b^l is the bias.

Then, the error propagated from the previous layer δ^{l+1} to the current layer δ^l can be computed by:

$$\delta^l = T^\top toep(W)^\top f'(z^l) \odot \delta^{l+1} \tag{11}$$

3.3.3 Testing

Because our model does not introduce any extra parameters or feature extraction modules, we only need to replace parameters in the CNN model with parameters trained by our model. The test architectures and all other settings are identical.

4. EXPERIMENTS

In this section, we evaluate our proposed transform-invariant CNN on several supervised learning tasks. First, to compare our model with state-of-the-art methods, we conduct experiments on the distorted versions of the MNIST handwriting dataset as in [18, 15]. The results in Section 4.1 show that TICNN is capable of achieving comparable or better classification performance with only raw input images and without adding any extra feature extraction modules or learnable parameters. Second, to test the improvement of TICNN on CNN for large-scale real-world image recognition tasks, we compare our model with AlexNet [21] on the ImageNet-2012

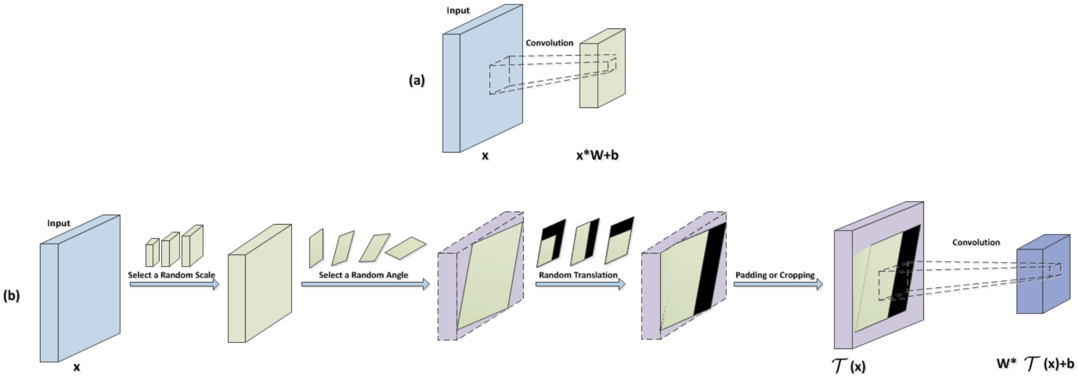

Figure 2: Detailed comparison of the structure of (a) convolution layer and the proposed (b) *transform-invariant* convolution layer. In (b), after convolving the inputs with the kernel, the output feature maps are transformed by a random rotation angle, scale factor, and translation proportion. Then, the randomly transformed feature maps are fed into the next layer.

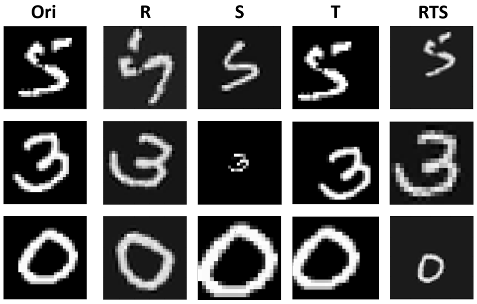

Figure 3: Examples of distorted MNIST dataset. Ori: raw images. R: rotated images. S: scaled images. T: translated images. RTS: images with scale, rotation and translation.

Method	R	S	T	RST
FCN	2.1	2.8	2.9	5.2
CNN	1.2	1.4	1.3	0.8
ST-CNN[15]	**0.8**	0.9	0.8	**0.6**
SI-CNN[18]	-	1.0	-	-
TI-CNN(ours)	**0.8**	**0.8**	**0.7**	**0.6**

Table 1: Classification error on the transformed MNIST dataset. The different distorted MNIST datasets are R: rotation, S: scale, T: translation, and RST: rotation-scale-translation. All models have the same number of parameters and use the same basic architectures.

dataset in Section 4.2. The results demonstrate that, with little degradation on the performance of classifying original test images, random transform can be applied to any layer in the CNN model and is able to consistently improve the performance on transformed images significantly. Finally, to evaluate the generalization ability of the TICNN model on other vision tasks with real-world transformations of images, we apply our model to solve the image retrieval task on the UK-Bench [26] dataset in Section 4.3. The improvement of retrieval performance reveals that the TICNN model has a good generalization ability and is better at solving real-world transformation varieties. We implement our method using the open source Caffe framework [16]. Our code and model will be available online.

4.1 MNIST

In this section, we use the MNIST handwriting dataset to evaluate all deep models. In particular, different neural networks are trained to classify MNIST data that have been transformed in various ways, including rotation (R), scale (S), translation (T), and rotation-scale-translation (RTS). The rotated dataset was generated from rotating MNIST digits with a random angle sampled from a uniform distribution $U[-90°, 90°]$. The scaled dataset was generated by scaling the digits randomly with a scale factor sampled from $U[0.7, 1.2]$. The translated dataset was generated from randomly locating the 28×28 digit in a 42×42 canvas. The rotated-translated-scaled dataset (RTS) was generated by randomly rotating the digit by $-45°$ to $-45°$, randomly scaling the digit by a factor ranging from [0.7, 1.2] and placing the digit at a location in a 42×42 image randomly, all with a uniform distribution. Some example images are presented in Fig. 3.

Following [15], all networks use the ReLU activation function and softmax classifiers. All CNN networks have a 9×9 convolutional layer (stride 1, no padding), a 2×2 max-pooling layer with stride 2, a subsequent 7×7 convolutional layer (stride 1, no padding), and another 2×2 max-pooling layer with stride 2 before the final classification layer. All CNN networks have 64 filters per layer. For the method in [18], convolution layers are replaced by scale-invariant layers using six scales from 0.6 to 2 at a scale step of $2^{1/3} = 1.26$. The spatial transformer module is placed at the beginning of the network [15]. In our random transform-invariant C-NN, the random transformation of the feature map module is applied to the second convolution layer, and *our model is only trained on the raw input images.* The rotation angle is sampled from $\mathcal{N}(0, 30^2)$, the scale factor is sampled from $\mathcal{N}(1, 0.15^2)$, and the translation proportion is sampled from $\mathcal{N}(0, 0.2^2)$.

All networks were trained with SGD for 150000 iterations, 256 batch size, 0.01 base learning rate, no weight decay,

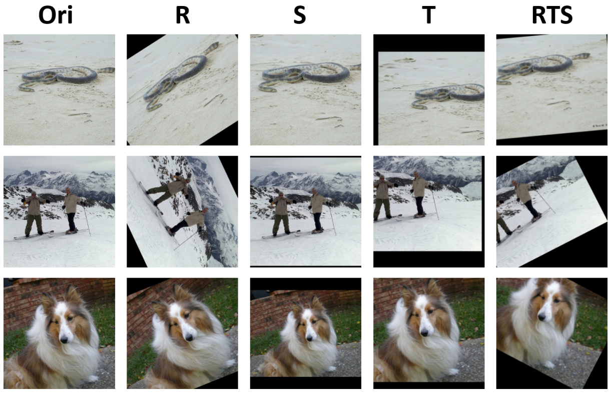

Figure 4: Distorted images in ImageNet. Ori: raw images. R: rotated images. S: scaled images. T: translated images. RTS: images with scale, rotation and translation.

and no dropout. The learning rate was reduced by a factor of 0.1 every 50000 iterations. The weights were initialized randomly, and all networks shared the same random seed.

The experimental results are summarized in Table 1. Please notice that we do not report the best result of ST-CNN [15], which was trained with a more narrow class of transformations selected manually (affine transformations).In our method, we did not optimize with respected to transformation classes. Therefore we compare with the most general ST-CNN defined for a class of projection transformations as in [22]. This table shows that our model achieves better performance on scale and translation and comparable performance on rotation and rotation-scale-translation. Because our model does not require any extra learnable parameters, feature extraction modules, or transformations on training images, the comparable performance still reflects the superiority of TICNN. In addition, the experimental results also indicate that the combination of convolution and pooling modules have some limitations on learning the invariance of rotation. Placing extra transformation modules at the beginning of the CNN is a more powerful way to compensate for this limitation.

4.2 ILSVRC-2012

The ILSVRC-2012 dataset was used for ILSVRC 2012 − 2014 challenges. This dataset includes images of 1000 classes, and it is split into three subsets: training (1.3M images), validation (50K images), and testing (100K images with held-out class labels). The classification performance is evaluated using two measures: the top-1 and top-5 errors. The former is a multi-class classification error. The latter is the main evaluation criterion used in ILSVRC and is defined as the proportion of images whose ground-truth category is not in the top-5 predicted categories. We use this dataset to test the performance of our model on large-scale image recognition tasks.

CNN models are trained on raw images and tested on both raw and transformed images. For all transform types, specific transformations are applied to the original images. Then, the transformed images are rescaled to have a 256 smallest image side. Finally, the center 224×224 crop is used for the test. The rotated (R) dataset was generated by randomly rotating the original images from -45° to 45° with a uniform distribution. The scaled dataset (S) was generated by scaling the original images randomly in $U[0.7, 1.5]$. The translated dataset (T) was generated by randomly shifting the image by a proportion of $U[-0.2, 0.2]$. For the rotation-scale-translation (RTS) dataset, all the aforementioned transformations were applied. Some examples of transformed images are presented in Fig. 4.

The architecture of our CNN model is the same as that of AlexNet [21]. This model consists of 5 convolution layers and 2 fully connected layers. The first convolution layer contains 96 kernels of size $11 \times 11 \times 3$. The second convolution layer contains 256 kernels of size $5 \times 5 \times 48$. The third convolutional layer contains 384 kernels of size $3 \times 3 \times 256$. The fourth convolutional layer contains 384 kernels of size $3 \times 3 \times 192$, and the fifth convolutional layer contains 256 kernels of size $3 \times 3 \times 192$. The fully connected layers have 4096 neurons each. Please refer to [21] for more details.

The model is trained for $450,000$ iterations. We use a base learning rate of 0.01 and decay it by 0.1 every $100,000$ iterations. We use a momentum of 0.9, weight decay of 0.0005, and a weight clip of 35. The convolutional kernel weights and bias are initialized by $\mathcal{N}(0, 0.01^2)$ and 0.1, respectively. The weights and bias of fully connected layers are initialized by $\mathcal{N}(0, 0.005^2)$ and 0.1. The bias learning rate is set to be $2\times$ the learning rate for the weights.

To investigate the influence of a random transformation module on the CNN model, we apply it to different convolution layers. The experimental results are summarized in Table 2 (test on raw validation set) and Table 3 (test on transformed validation set). Some key insights obtained from the results are listed as follows:

- In general, when random transforms are applied to feature maps of higher layers in the CNN model, the recognition performance on both the original dataset and transformed dataset tends to be better. A possible explanation for this result is that representations extracted by lower layers are elementary features; they are related to a very precise location and have a very high resolution. Feature maps with higher resolution will be considerably more sensitive to transformations and noise, and location changes in lower-level feature maps could lead to a significant change in their visual pattern. Therefore, when a random transform is applied to feature maps of lower layers, it could be very difficult for the model to infer the original image content. Consequently, the useful information that the model can efficiently learn from each sample is reduced.

- By incorporating a random transformation, the model can still obtain comparable or even better performance than the CNN model on raw test images; this phenomenon shows that this randomness can prevent overfitting. Notably, the performance on transformed images is significantly improved on all transformation types (rotation, translation, scale, and rotation-translation-scale), indicating that TICNN improves the generalization ability of the CNN model on transformation variances.

- Applying our random transform module on the image data layer is identical to unlimited data augmentation. Models with random transformations on the

Model	R	T	S	RTS
CNN+Data Augmentation	56.3/79.7	56.3/79.4	55.6/78.9	56.6/79.8
TI-Conv1	55.0/78.4	56.6/79.7	56.2/79.1	56.5/79.4
TI-Conv2	56.1/79.3	56.5/79.7	56.2/79.3	56.6/79.7
TI-Conv3	56.7/79.6	56.9/79.9	56.4/79.4	57.0/80.0
TI-Conv4	57.1/80.1	57.2/80.1	56.7/79.5	56.9/79.9
TI-Conv5	57.1/80.2	**57.6/80.5**	57.0/80.0	57.1/80.0
TI-Conv1,2,5	57.2/80.2	57.5/80.4	57.1/80.2	57.2/80.3
SI-CNN	57.3/80.3			
CNN	57.1/80.2			

Table 2: Classification accuracy on the ILSVRC-2012 validation set (raw). TI-Conv$i$ indicates that we apply random transformations on the feature maps of layer i. R, T, S, and RTS represent rotation, translation, scale, and rotation-scale-translation, respectively.

Model	R	T	S	RTS
CNN+Data Augmentation	36.5/58.3	50.0/73.9	54.0/77.6	36.0/58.2
TI-Conv1	35.7/57.9	50.5/74.4	54.0/77.5	35.6/58.0
TI-Conv2	36.1/58.2	49.9/74.0	53.9/77.5	35.5/57.8
TI-Conv3	36.8/58.9	50.0/74.2	54.6/77.9	36.3/58.9
TI-Conv4	37.2/59.5	50.3/74.3	54.5/77.7	36.2/58.9
TI-Conv5	37.1/59.2	50.1/74.6	54.7/78.0	36.0/58.7
TI-Conv1,2,5	**37.3/60.2**	**51.3/75.4**	**55.0/78.5**	**37.5/60.5**
SI-CNN	-	-	53.8/77.3	-
CNN	36.6/57.7	46.5/70.8	53.3/76.9	33.3/55.2

Table 3: Classification accuracy on the transformed ILSVRC-2012 validation set. TI-Conv$i$ indicates that we apply random transformations on the feature maps of layer i. R, T, S and RTS represent rotation, translation, scale, and rotation-translation-scale, respectively.

image data layer are worse than models with random transformations on the convolutional layer, revealing that TICNN model is better than simple image data augmentation.

- Comparing Table 2 with Table 3, we can observe that the performance of CNN models significantly decreases when faced with transformations. The combination of convolution operations and pooling operations shows limited capacity for transform invariance. We need to add more powerful modules into current CNNs in the future.

Effect on Feature Detectors. We evaluate the transform invariance achieved by our model using the invariance measure proposed in [12]. In this approach, a neuron is considered to be firing when its response is above a certain threshold t_i. Each t_i is chosen to satisfy the condition that $G(i) = \sum |h_i(x) > t_i|/N$ is greater than 0.01, where N is the number of inputs. Then *local firing rate* $L(i)$ is computed as the proportion of transformed inputs that a neuron fires to. To ensure that a neuron is selective and with a high local firing rate (invariance to the set of the transformed inputs), the invariance score of a neuron is computed by the ratio of its invariance to selectivity, i.e., $L(i)/G(i)$. We report the average of the top 20% highest scoring neurons ($p = 0.2$) as in [18]. Please refer to [12] for more details.

Here, we construct the transformed dataset by applying rotation ($[-45°, 45°]$ with step size 9°), scale ($[0.7, 1.5]$ with step size 0.08) and translation ($[-0.2, 0.2]$ with step size 0.04) on the 50,000 validation images of ImageNet-2012. Fig. 5 shows the invariance scores of CNN (AlexNet) and TICNN (TI-Conv1,2,5) measured at the end of each layer. We can observe that by applying random transformation on feature maps during training, TICNN produces features that are more transform invariant than those from CNN models.

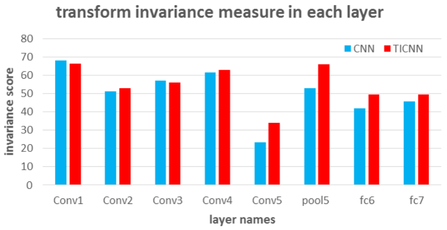

Figure 5: Transform invariance measure (the larger the better).

Some Examples. Figure 6 shows some test cases in which CNN is unable to predict correct labels for the input images while TICNN generates true predictions. They demonstrate that TICNN is more robust than the CNN model.

4.3 UK-Bench

We also evaluate our TICNN model on the popular image retrieval benchmark dataset UK-Bench [26]. This dataset includes 2550 groups of images, each containing 4 relevant samples about one certain object or scene from different

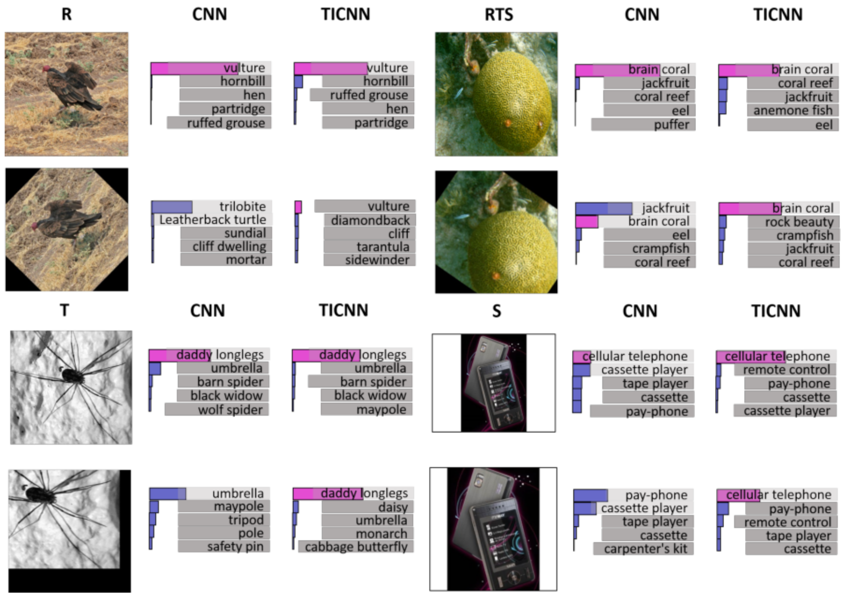

Figure 6: Some ImageNet test cases with the 5 most probable labels as predicted by AlexNet and our model. The length of the horizontal bars is proportional to the probability assigned to the labels by the model. Pink indicates ground-truth. The transformations applied to input images are rotation (R), scale (S), translation (T), and rotation-scale-translation (RTS).

Model	UK-Bench	UK-Bench+MIRFlickr
TICNN (R)	**3.572**	**3.483**
TICNN (T)	3.536	3.452
TICNN (S)	3.551	3.461
TICNN (RTS)	3.561	3.479
CNN	3.518	3.350
SIFT	3.350	3.295

Table 4: Performance of the TICNN and CNN models on the UK-Bench retrieval dataset. TICNN has the same architecture as AlexNet. R, T, S and RT-S represent ration, translation, scale, and rotation-translation-scale, respectively.

viewpoints. Each of the total 10200 images is used as one query to perform image retrieval targeting at finding all its 3 counterparts. We choose UK-Bench because the viewpoint variation in the dataset is very common. Although many of the variation types are beyond the three types of geometry transformations that we attempt to address in this paper, we demonstrate the effectiveness of TICNN for solving many severe rotation, translation and scale variance cases in image retrieval tasks. To test the CNNs in a dataset with larger scale, we also add the $1M$ images in MIR Flickr [13] as negative examples.

For feature extraction, we follow the practice proposed in [37] to feed each image into the TICNN and CNN models, and we perform average pooling on the last pooling layer to obtain a compact feature representation. Specifically, we apply the AlexNet architecture for the baseline CNN model and the TICNN model, of which the fifth pooling layer generates a $13 \times 13 \times 256$ shape response map. We obtain the average values for each of the 256 channels and obtain a 256-dimensional feature for every image. Subsequently, we compute the root value of each dimension and perform $L2$ normalization.

To perform image retrieval in UK-Bench, the Euclidean distances of the query image with respect to all 10200 database images are computed and sorted. Images with the smallest distances are returned as top ranked images. The NS-Score (average top four accuracy) is used to evaluate the performance, and a score of 4.0 means that all the relevant images are successfully retrieved in the top four results.

In the evaluation, we compare our TI-Conv1,2,5 model with the AlexNet model trained on ImageNet. As shown in Table 4, TICNN achieves a considerable performance improvement. After carefully analyzing the retrieved results, we find that our model successfully solves multiple transformation cases in the retrieval task. In Fig. 7, we illustrate six positive cases in which TICNN outperforms the baseline in Figs. 7(a)-7(f), and we also provide two negative cases in Fig. 7(g)-7(h).

As shown in Fig. 7(a), the CNN model only retrieves one relevant image, while TICNN retrieves another one as shown in the bottom row. The additionally returned database image has an obvious scale transformation with respect to the query, and it is successfully retrieved as the most similar one in the database by our model. As shown in Fig. 7(b) and Fig. 7(c), our model also performs better for rotation variance than CNN. In Fig. 7(d) and Fig. 7(e), the objects (the road sign and basketball) appear in different scales and different spatial locations, which impacts the performance of CNN but is well handled by TICNN.

Regarding the failure cases of TICNN shown in Fig. 7(g), our model returns a false positive sample as shown in the third column of the bottom row. We observe that this false

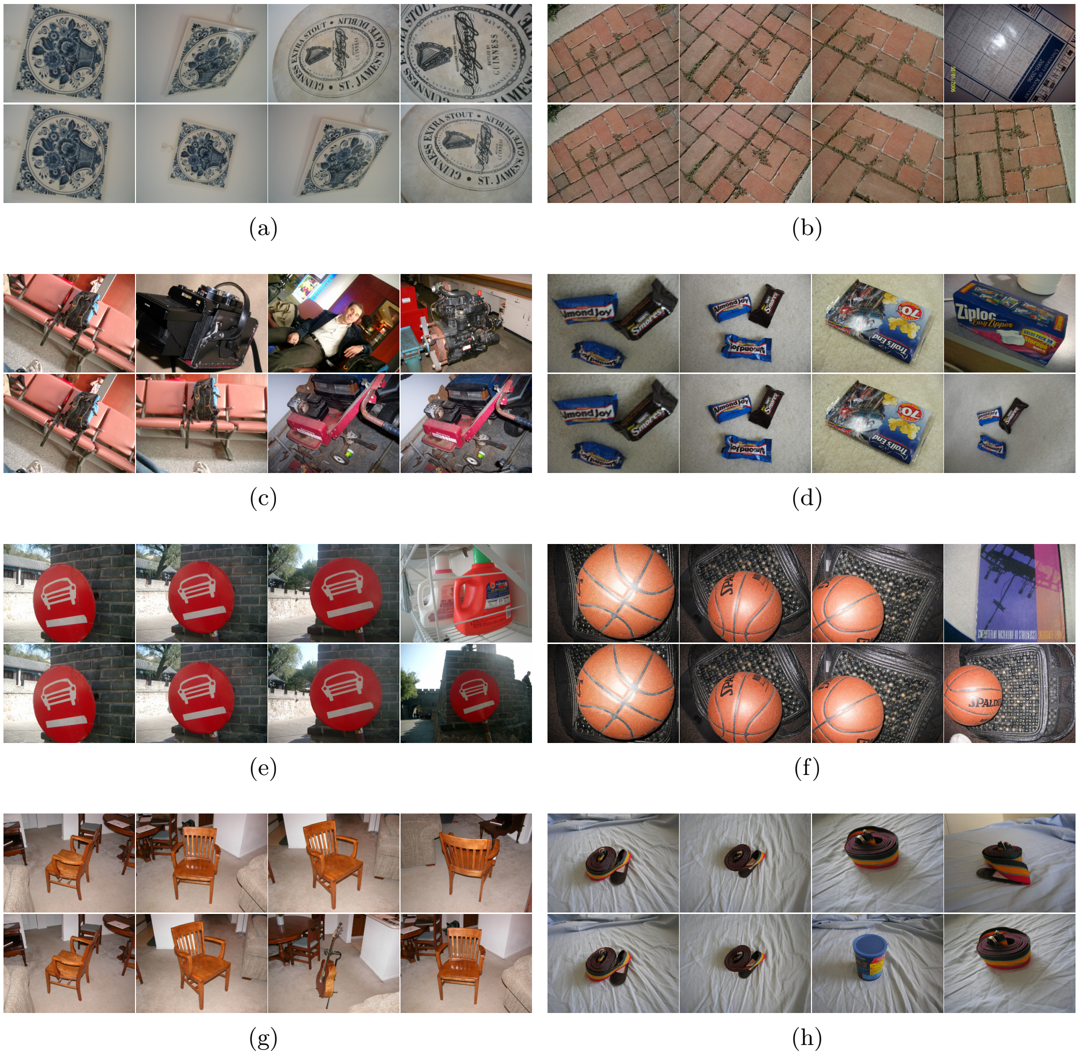

(a) (b) (c) (d) (e) (f) (g) (h)

Figure 7: Top 4 retrieval results on the UK-Bench dataset with the CNN and TICNN models. In each group, the results of the CNN model and TICNN model are given in the top and bottom row, respectively. The results in (a)-(f) are positive cases, whereas (g)-(h) show two failure cases.

positive image also contains a chair like the query, but it appears in different scales and locations, which leads to a false match. Some other failure cases are similar to that in Fig. 7(h), where a large 3D viewpoint variance occurs, which is impossible to be produced in our training phase.

5. CONCLUSIONS

In this paper, we introduce a very simple and effective approach to improve the transform invariance of CNN models. By randomly transforming the feature maps of CNN layers during training, the dependency of the specific transform level of the input is reduced. Our architecture is different from that of previous approaches because we improve the invariance of deep learning models without adding any extra feature extraction modules, any learnable parameters or any transformations on the training dataset. Therefore, the transform invariances of current CNN models are very easy to be improved by just replacing their corresponding weights with our trained model. Experiments show that our model outperforms CNN models in both image recognition and image retrieval tasks.

Acknowledgments This work is supported by NSFC under the contracts No.61572451 and No.61390514, the 973 project under the contract No.2015CB351803, the Youth Innovation Promotion Association CAS CX2100060016, Fok Ying Tung Education Foundation, Australian Research Council Projects: DP-140102164, FT-130101457, and LE140100061.

6. REFERENCES

[1] J. M. Alvarez, Y. LeCun, T. Gevers, and A. M. Lopez. Semantic road segmentation via multi-scale ensembles of learned features. *ECCV Workshop on Computer Vision in Vehicle Technology: From Earth to Mars*, 2012.

[2] J. Bruna and S. Mallat. Invariant scattering convolution networks. *IEEE Trans. Pattern Anal. Mach. Intell.*, 35:1872–1886, 2013.

[3] T. S. Cohen and M. Welling. Transformation properties of learned visual representations. *ICLR*, 2015.

[4] J. Donahue, L. A. Hendricks, S. Guadarrama, M. Rohrbach, S. Venugopalan, K. Saenko, and T. Darrell. Long-term recurrent convolutional networks for visual recognition and description. *CVPR*, 2015.

[5] H. Fang, S. Gupta, F. Iandola, R. Srivastava, L. Deng, P. Dollar, J. Gao, X. He, M. Mitchell, J. C. Platt, L. Zitnick, and G. Zweig. From captions to visual concepts and back. *CVPR*, 2015.

[6] C. Farabet, C. Couprie, L. Najman, , and Y. LeCun. Learning hierarchical features for scene labeling. *IEEE Trans. Pattern Anal. Mach. Intell*, 2013.

[7] C. Gan, N. Wang, Y. Yang, D.-Y. Yeung, and A. G. Hauptmann. Devnet: A deep event network for multimedia event detection and evidence recounting. In *CVPR*, pages 2568–2577, 2015.

[8] C. Gan, T. Yang, and B. Gong. Learning attributes equals multi-source domain generalization. *CVPR*, 2016.

[9] C. Gan, T. Yao, K. Yang, Y. Yang, and T. Mei. You lead, we exceed: Labor-free video concept learning by jointly exploiting web videos and images. *CVPR*, 2016.

[10] R. Gens and P. M. Domingos. Deep symmetry networks. *NIPS*, 2014.

[11] R. G. Georgia Gkioxari and J. Malik. Contextual action recognition with r*cnn. *ICCV*, 2015.

[12] I. J. Goodfellow, Q. V. Le, A. M. Saxe, H. Lee, and A. Y. Ng. Measuring invariances in deep networks. *NIPS*, 2009.

[13] M. J. Huiskes and M. S. Lew. The mir flickr retrieval evaluation. In *MIR*. ACM, 2008.

[14] E. S. J. Long and T. Darrell. Fully convolutional networks for semantic segmentation. *CVPR*, 2015.

[15] M. Jaderberg, K. Simonyan, A. Zisserman, and K. Kavukcuoglu. Spatial transformer networks. *NIPS*, 2015.

[16] Y. Jia, E. Shelhamer, J. Donahue, S. Karayev, J. Long, R. Girshick, S. Guadarrama, and T. Darrell. Caffe: Convolutional architecture for fast feature embedding. *arXiv preprint arXiv:1408.5093*, 2014.

[17] S. R. Kaiming He, Xiangyu Zhang and J. Sun. Deep residual learning for image recognition. *CVPR*, 2016.

[18] A. Kanazawa and A. Sharma. Locally scale-invariant convolutional neural networks. *NIPS*, 2014.

[19] A. Karpathy and L. Fei-Fei. Deep visual-semantic alignments for generating image description. *CVPR*, 2015.

[20] J. J. Kivinen and C. K. I. Williams. Transformation equivariant boltzmann machines. In *Artificial Neural Networks and Machine Learning*, pages 1–9, 2011.

[21] A. Krizhevsky, I. Sutskever, and G. E. Hinton. Imagenet classification with deep convolutional neural networks. *NIPS*, pages 1097–1105, 2012.

[22] D. Laptev, N. Savinov, J. M. Buhmann, and M. Pollefeys. Ti-pooling: transformation-invariant pooling for feature learning in convolutional neural networks. In *CVPR*, 2016.

[23] Q. V. Le, J. Ngiam, Z. Chen, D. J. hao Chia, P. W. Koh, and A. Y. Ng. Tiled convolutional neural networks. *NIPS*, 2010.

[24] Y. Lecun, L. Bottou, Y. Bengio, and P. Haffner. Gradient-based learning applied to document recognition. In *Proceedings of the IEEE*, pages 2278–2324, 1998.

[25] K. Lenc and A. Vedaldi. Understanding image representations by measuring their equivariance and equivalence. *CVPR*, 2015.

[26] D. Nister and H. Stewenius. Scalable recognition with a vocabulary tree. In *CVPR*, pages 2161–2168, 2006.

[27] S. Nitish, H. Geoffrey, K. Alex, S. Ilya, and S. Ruslan. Dropout: A simple way to prevent neural networks from overfitting. *Journal of Machine Learning Research*, pages 1929–1958, 2014.

[28] Y. Pan, T. Mei, T. Yao, H. Li, and Y. Rui. Joint modeling embedding and translation to bridge video and language. *CVPR*, 2016.

[29] S. Richard. *Computer Vision: Algorithms and Applications.* 2010.

[30] P. Sermanet and Y. LeCun. Traffic sign recognition with multi-scale convolutional networks. *IJCNN*, 2011.

[31] K. Simonyan and A. Zisserman. Two-stream convolutional networks for action recognition in videos. *NIPS*, 2014.

[32] K. Simonyan and A. Zisserman. Very deep convolutional networks for large-scale image recognition. *CoRR*, abs/1409.1556, 2014.

[33] K. Sohn and H. Lee. Learning invariant representations with local transformations. In *ICML*, 2012.

[34] K. Sohn and H. Lee. Understanding image representations by measuring their equivariance and equivalence. *CVPR*, 2015.

[35] C. Szegedy, W. Liu, Y. Jia, P. Sermanet, S. Reed, D. Anguelov, D. Erhan, V. Vanhoucke, and A. Rabinovich. Going deeper with convolution. *CVPR*, 2015.

[36] Z. Wang, J. Yang, H. Jin, E. Shechtman, A. Agarwala, J. Brandt, and T. S. Huang. Deepfont: Identify your font from an image. In *ACM MM , 2015*, pages 451–459, 2015.

[37] L. Xie, L. Zheng, J. Wang, A. Yuille, and Q. Tian. Interactive: Inter-layer activeness propagation. In *CVPR*, 2016.

[38] L. Yao, A. Torabi, K. Cho, N. Ballas, C. Pal, H. Larochelle, and A. Courville. Describing videos by exploiting temporal structure. *ICCV*, 2015.

[39] L. Zheng, S. Wang, Z. Liu, and Q. Tian. Packing and padding: Coupled multi-index for accurate image retrieval. In *CVPR*, pages 1939–1946, 2014.

[40] L. Zheng, S. Wang, L. Tian, F. He, Z. Liu, and Q. Tian. Query-adaptive late fusion for image search and person re-identification. In *CVPR*, pages 1741–1750, 2015.

[41] L. Zheng, S. Wang, J. Wang, and Q. Tian. Accurate image search with multi-scale contextual evidences. *International Journal of Computer Vision*, pages 1–13, 2016.